PROPERTIES OF NANOSTRUCTURED COMPOSITE TITANIUM COATING ON ALUMINIUM SURFACE

Yu. Tyurin[1], O. Ivanov[2], O. Kolisnichenko[1], M. Kovaleva[2], I. Duda[1], O. Maradudina[2], Y. Trusova[2]

1 E.O.Paton Electric Welding Institute, Ukraine
2 Belgorod State University, Russia

ABSTRACT

Composite coatings of titanium powder were deposited on aluminium samples by using the cumulative-detonation equipment. Consumption of fuel mixture components (propane-oxygen-air) was up to 4.3 m^3 per kilo of a coating. The coatings were examined by scanning electron microscopy (SEM), transmission electron microscopy (TEM) with diffraction, X-ray phase analysis, hardness measurements, as well as plasticity and adhesion/cohesion resistance scratch tests. It is shown that the coatings are characterised by the presence of nanodispersed ceramic formations, and feature high values of plasticity, hardness and adhesion strength.

Key words: cumulative-detonation equipment,nanocomposite, coating, hardness, nanodispersed ceramic.

INTRODUCTION

Wear and corrosion of the aluminium skin of aircraft begin as early as after two years of operation under severe climatic conditions, despite the use of the most advanced protection methods [1]. The applied protective coatings should be guarded against mechanical damages, scratches, nicks, etc. The points of damages, as well as zones affected by exhaust engine gases, acid vapours and other aggressive environments may act as centres of initiation of corrosion, which particularly actively develops in locations of accumulation of moisture and dirt [2]. In this connection, development of wear- and corrosion-resistant coatings to be applied to the surface of the aircraft skin is an issue of primary importance. The challenge now is to protect surfaces of the aluminium parts under the most severe atmospheric conditions for a term of not less than 6-8 years [1-2].

In view of high physical-mechanical properties of titanium and its compounds, it is of interest to deposit a coating of titanium-base composite materials on aluminium. A thin layer of the titanium-base coating will have no substantial effect on weight of a structure. While applying the coating, it is necessary to take into account that aluminium structures operate under cyclic loading conditions. This imposes increased requirements not only to strength and adhe-

sion of the coating to the aluminium substrate, but also to the probability of its weakening in realisation of the technology.

At present the titanium coatings are produced by plasma spraying of wire VT1-0. The coatings are porous and have low adhesion. The maximal values of adhesion (up to 80 MPa) are achieved at a substrate temperature of 500 ^{o}C. The substrates are made from alloys VT6 and VT 20 [3]. Much work is underway now on using upgraded HVOF [4, 5], as well as a helium jet under a pressure of 24 atm. and temperature of 450-550 ^{o}C [6], or a nitrogen jet under a pressure of 30 atm. and temperature of up to 600 ^{o}C [7]. The titanium coatings are produced by using plasmatrons [8]. It can be noted that all the coatings are porous, their adhesion strength is not in excess of 30 – 50 MPa, and they comprise local phases with hardness of HV 700 - 1500. These phases contain nitrogen, oxygen and carbon.

The purpose of this study is to develop a power-saving technology and equipment for deposition of protective titanium powder coatings on surfaces of aluminium parts. The main problem is to provide a high adhesion to the substrate and eliminate loss in strength of the aluminium part surfaces.

METHODS OF SAMPLE MANUFACTURING AND ANALYSIS

The power-saving cumulative-detonation device for deposition of titanium powder coatings was developed to address the above problem. The device provides a high velocity of the powder materials (> 800 m/s) without its overheating. Because of a high kinetic energy, the powder material is deformed and diluted with the surface layer of the aluminium substrate. This allows formation of thin coatings and hardening of the aluminium layer under a coating.

The device provides formation of quality coatings at a 20 times lower consumption of power and 5-10 times lower consumption of fuel gas mixture components, compared with known HVOF devices [9].

An essential difference of the cumulative-detonation device from the detonation one is that it combines the energy from several, specially profiled detonation chambers. This provides an efficient energy transfer to the powder materials. In addition, it is characterised by a wide possibility of controlling the velocity and temperature of the powder materials. The device operates at a frequency of up to 30 Hz, this allowing the use of standard powder and gas control devices, simplification of the equipment, reduction of its price, and improvement of its operational reliability.

The cumulative-detonation technology is of a pulse character. This makes it possible to form coatings from a small distance (10-60 mm) in a shielding gas atmosphere. As a result, oxidation and losses of spraying materials are reduced. The titanium powder utilisation factor in deposition of coatings is 85 - 90 %. The velocity of the powder material is 800 – 900 m/s.

The coating was deposited under conditions given in *Table 1*.

Table 1– Flow rate of gas and consumption of powder in cumulative-detonation device per kilo of a coating

Expenditure					
Ti, Kg/h	$C_3H_8+O_2$, m^3	C_3H_8 m^3/h	O_2 m^3/h	Air m^3/h	G_{O2}/G_{C3H8}
1,1	2,84	0,536	2,303	1,466	4,84

The distance from the nozzle section to a specimen was 30 mm. Specimens of an alloy consisting of Al as a base, 0.3 % Mn and 8 % Mg were used as a substrate. A uniform coating 130 μm thick was deposited on the specimen surface.

The coating was deposited by using the Sumitomo Titanium Corp. titanium powder. As shown by the investigation results, the powder particles were 1 to 50 μm in size, and the powder consisted of 100 wt. % Ti (*Fig. 1*).

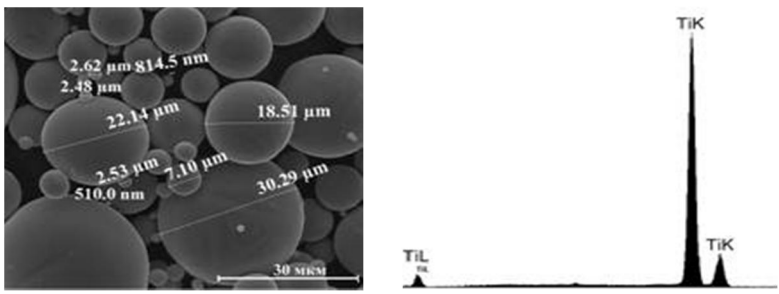

a) b)

Fig. 1– a) Morphology and (b) elemental composition (energy dispersive spectrum) of titanium powder

Examinations of the powder were carried out by using electron ion microscope Quanta 200 3D equipped with integrated microanalysis system Pegasus 2000.

Local phase and diffraction analysis of the titanium coating was conducted by using transmission electron field emission microscope Tecnai G2 20F S-T (FEI) with microdiffraction and X-ray powder diffractometer ARL X'TRA, providing integrated information on a layer of several microns thick. X-ray diffraction analysis of the coating was carried out in the pseudo-parallel beam mode in an angle range of 18 - 85°2θ.

RESULTS AND DISCUSSION

Examinations of elemental composition of the coating were carried out at a depth of several microns from the surface. The resulting spectra show the presence of oxygen, aluminium, titanium and carbon in the coating (*Fig. 2*).

The coating is 130 μm thick, which is commensurable with diameter of the coarsest titanium particles equal to 45.48 μm (see *Fig. 1*). It can be assumed that the titanium particles, upon colliding with the substrate, deform its surface layer to form aluminium splashes, which are localised in the coating, thus providing the aluminium content of the coating equal to 0.58 wt. % (*Fig. 2*).

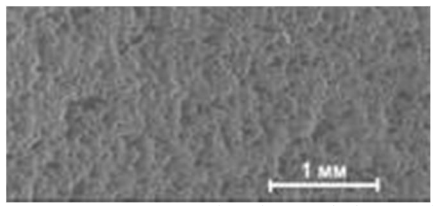

	Wt %/ At %
Ti	62,6/ 34,5
Al	0,5 /0,5
O	27,3/ 44,3
C	9,4/20,5

Fig. 2– Appearance of surface and elemental composition of titanium coating

As shown by examinations of microstructure and elemental composition of transverse section of a coated sample (*Fig. 3*), the coating is uniform and dense, and has a good adhesion to the substrate. The bulk of the coating material is deformed and closely packed. However, coarse inclusions in the form of non-deformed discrete particles are detected (see *Fig. 3*).

Qualitative evaluation of the coating to basemetal adhesion strength, according to GOST 9.304-87, showed that adhesion corresponded to a maximal point – 1. Moisture absorption by the coating was 0.90 mg/cm^2 (GOST 4650-80, method A), which corresponded to porosity below 1 %.

Titanium has low thermal conductivity (22.07 W/mK), which hampers heating and deforming it in formation of a coating. It is likely that coarse particles (> 30 μm) were not heated and, despite a high kinetic energy, were deformed only slightly. At the same time, they hardened the substrate material and consolidated the underlying coating layers.

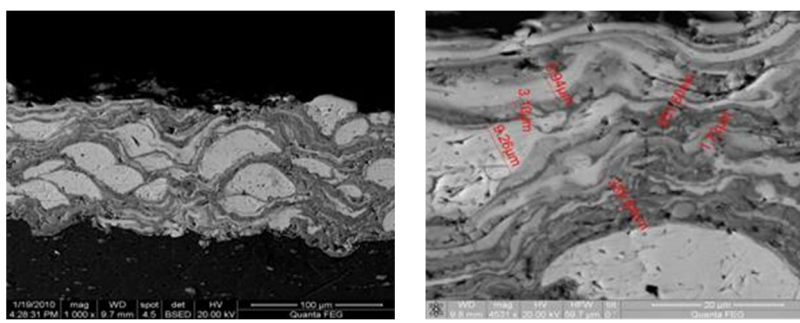

Fig. 3– Microstructure of transverse section of coated sample.

The analysis performed allows a conclusion that the fine powder particles were heated and deformed to a state of fine lamellae, and that they filled up the spacings between the coarse particles to form a dense coating (see Fig. 3). Thickness of the lamellae in the coating was 100-1000 nm.

Investigation of the coating to substrate adhesion zone showed that the visible interface was free from defects. The mixed structure consisting of coating islands in aluminium, having different shapes and sizes, can be clearly seen in the titanium and aluminium contact zone (*Fig. 4, Table 2*). Part of the powder material (titanium) penetrated deep into the substrate material to form a strong bond with it.

Table 2– Analysis of elemental composition of coating and substrate, see Figure4a

Point	Wt % / At %				
	Ti	Al	O	Mn	Mg
1	99,1/ 98,4	0,8/ 1,5	-	-	-
2	74,6/ 51,3	2,5/ 1,5	22,8/ 47,1	-	-
3	-	92,3/91,9	-	0,7/ 0,3	6,9/ 7,7

Analysis of elemental composition of regions adjoining the interface between the coating and substrate showed the presence of titanium and up to 0.86 wt. % aluminium at point 1 (see *Fig. 4*).

Point 2 is an interface between the coating material and substrate. This region formed as a result of interaction of heated titanium, working gas components and substrate material. The analysis results prove the presence of the substrate and coating materials in the transition region. This region contains oxygen, titanium and aluminium. Region 3 contains aluminium and aluminium alloying elements, i.e. magnesium and manganese. The investigation conducted confirms the hypothesis of dilution of the coating material, i.e. titanium, with the substrate material, i.e. aluminium. It was established that hardness of the fine lamellae in the coating was $HV_{0.01}$ 1595, this being 2 - 3 times higher than that of the aluminium substrate material (point 2 and coarse titanium particles, *Fig. 5*).

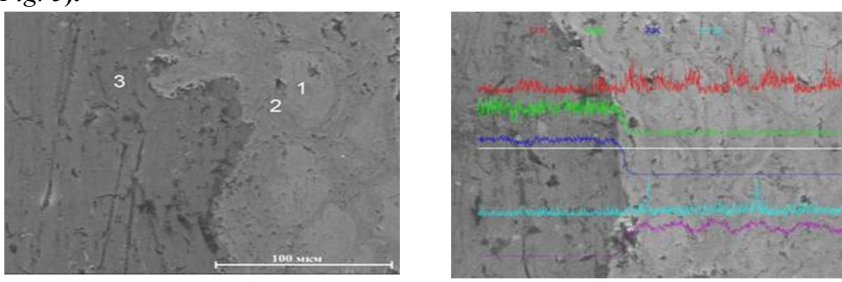

a) b)

Fig. 4– Microstructure of titanium coating on aluminium: a – points of measuring elemental composition; b – analysis of elemental composition of coating and substrate

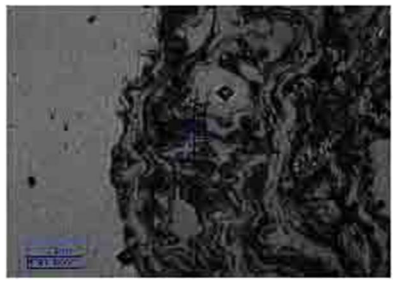

Fig. 5– Structure and hardness $HV_{0.01}$: 1595 of fine lamellae, 346 of titanium particles, 303 of interfac

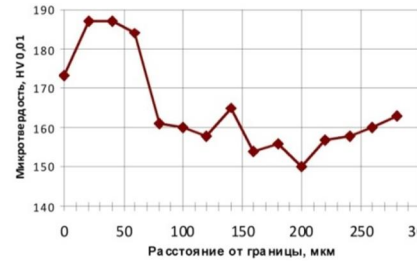

Fig. 6– Hardness of aluminium substrate layer

A titanium particle with maximum size of 40 μm can be seen in the Figure. This particle has hardness $HV_{0.01}$ 346. Hardness of the material at the interface is $HV_{0.01}$ 303. And hardness of the aluminium substrate under the coating varies to a depth of 100 μm from $HV_{0.01}$ 190 to an average hardness of the sample material equal to $HV_{0.01}$ 160 (*Fig. 6*).

Local phase and structure analysis of the coating material showed that lamellae in the coating consisted of the dislocation-free titanium nanocrystalline grains 30 nm in size, separated by interlayers of the amorphous phase (C, Al) (*Fig. 7a*), and titanium oxide crystalline grains with cubic lattice (*Fig. 7b*).This is confirmed by results of X-ray phase and diffraction analysis of the coating (*Fig. 8*).

The phase analysis shows that the main phase in the coating layer is Ti with face-centred close-packed structure (a = 2.965 Å). The presence of other phases was determined from reflexes in an angle range of 10 to 40°(see *Fig. 8*)**.**

Some lines are overlapped in this range, which makes the phase analysis more difficult to conduct. The distinguished interplanarspacings calculated from reflexes make it possible to identify the following phases in the coating: TiC with cubic lattice (a = 4.349 Å), and TiO with cubic lattice (a = 4.027 Å).

Complex phases in interplanarspacings have an amorphous structure, which is proved by the transmission electron microscopy results. This structure could be caused by a high-temperature cycle in formation of the coating [10-11].

Therefore, it can be assumed that the values of hardness in a layer at the interface with the substrate and in fine lamellae of the coating are attributable to the absence of dislocations inside the crystalline grains and ratio of the volume contents of nanocrystalline to amorphous phases of metallic and non-metallic titanium compounds.

Strength of intermediate and near-interface layers leads to increase of deformation resistance of the coating.

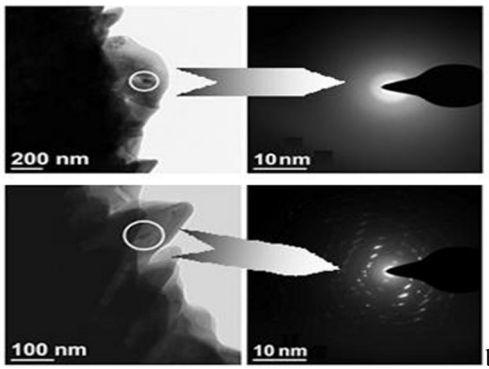

Fig. 7– Diffraction PEM photographs of material of lamellae in coating: a – amorphous phases (C, Ti, Al); b – titanium oxide crystalline grains with cubic lattice

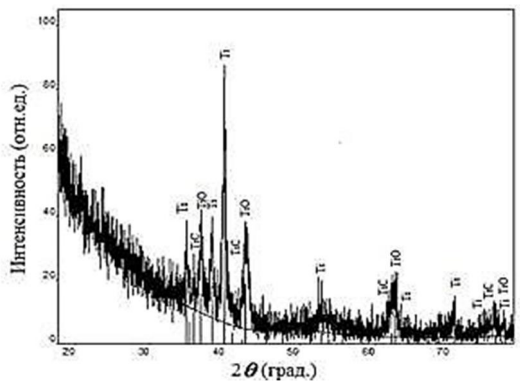

Fig. 8– Region of diffraction pattern of titanium powder coating

The absence of dislocations inside the crystalline grains leads to increase in elasticity and, at the same time, in plasticity of the coatings. It was detected for the first time ever [12], as far back as 20 - 25 years ago, that ceramic materials of titanium oxides acquire superplastic properties at room temperature at the characteristic sizes of crystals equal to several nanometres.

Plasticity of the coating material is confirmed by investigations of adhesion/cohesion strength using scratch tester REVETEST (CSM Instrumens) [12 - 13]. The similar procedure was employed to determine adhesion and cohesion of thermal spray nickel-base coatings [14]. The device made scratches on the coatings with a spherical diamond indenter of the "Rockwell C" type with a rounding radius of 200 μm at a continuously growing load in a range of 0.9-200 N. Physical parameters, such as acoustic emission, friction coefficient and indenter penetration depth, were fixed. Minimal (critical) load Lc, which led to fracture of the coatings, was determined as a result. Conditionally, the process of fracture of the coating in scratching can be subdivided into five stages (*Fig. 9*). The indenter monotonously penetrates into the coating within a load range of 0.9 to 8 N: the friction coefficient increases but very slightly, and the acoustic emission signals remain unchanged. Under a load of 8 N the indenter completely penetrates into the coating. The diamond indenter slides over the coating at a friction coefficient of 0.65 - 0.55.

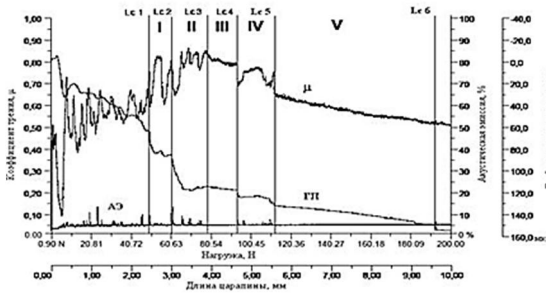

Fig. 9– Dependences of acoustic emission (AE), friction coefficient (μ) and indenter penetration depth (PD) on applied load in scratch tests

Further movement of the indenter and increasing of load (49.6 - 60.6 N) cause expulsion of the coating material ahead of the indenter in the form of humps and increase of the indenter penetration depth (stage I). Overcoming of humps by the indenter is accompanied by growth of the friction coefficient (up to 0.7) and formation of acoustic emission peaks (see *Fig. 9*).

Sudden change in the indenter penetration depth (~ 120 μm) and friction coefficient (0.8) occurs at a load in the 60.6 – 78.5 N range (stage II), this being caused by pushing off of the coating material and deformation of the substrate. Thickness of the coating was 130 μm (see *Fig. 3a*).

Increasing the load to more than 78.5 N (stage III) leads to impression of the coating material into the substrate and sliding of the indenter over the groove bottom into the coating without a change in its penetration depth (no variations in the acoustic emission signals were fixed).

As the load is increased, the coating is impressed into the substrate material (stage IV), which is accompanied by formation of herring-bone (transverse) cracks on the groove bottom and intensive cohesive destruction of the coating material (load – 93.4 N). Increasing the load from 112.5 to 184.3 N (stage V) at monotonous sliding of the indenter causes plastic deformation of the coating, thinning and impressing it into the substrate material.

The almost complete absence of peaks on the acoustic emission curve confirms plasticity of the coating and its deformation without cracks and delaminations.

The loss of the coating to substrate adhesion strength was fixed from a dramatic increase in the indenter penetration depth (~ 160 μm), a small jump of the acoustic emission signals and elemental analysis of traces of deformation by the diamond indenter under a load of 184.3 N (Fig. 10).The elemental analysis of a trace of deformation showed that the groove bottom comprised regions with a titanium content of up to 9.4 wt. %, and regions where the coating was impressed into the substrate material and which contained up to 97.6 wt. % Ti (*Table 3*).

Table 3– The elemental analysis

Point	Wt % / At %		
	Ti	Al	Mg
1	9,4/ 5,5	84/ 87,1	6,5/ 7,4
2	97/ 95,6	1,7/ 3,1	0,7/ 1,3

Therefore, the loss of the cohesion strength of the coating at a load on the indenter equal to 93 N, and the loss of the coating to substrate adhesion strength at a load of 184.3 N were fixed. The coating adhesion strength can be estimated from the formula [13] used for vacuum coatings:

$$\sigma = L / 2\omega(Dd)^{1/2} \quad (1)$$

Where L is the load on the indenter, N; ω is the groove width, μm; D is the diameter of the spherical diamond indenter, m and d is the scratch depth, m. The experiment on evaluation of the coating adhesion strength was carried out by scratching the coating under constant load L = 190 N. The groove with mean width ω = 677 μm was formed as a result. The scratch had depth d = 160 μm, which is more than the coating thickness.

CONCLUSIONS

The cumulative detonation technology and equipment provide deposition of coatings from titanium powder (particle size 5 – 50 μm) on aluminium at a deposition efficiency of 1 kg per hour and consumption of fuel mixture components equal to 3.5 m^3 per kilo of a coating.

As shown by the investigations, the coatings consist of deformed particles of titanium and compounds of titanium with oxygen and carbon. These materials have either amorphous or nanocrystalline structure, high plasticity and hardness of up to $HV_{0.01}$ 1595.

It was noted that hardness of the aluminium substrate layer in formation of a coating increased to $HV_{0.01}$ 190, and then gradually decreased to $HV_{0.01}$ 160 at a depth of more than 100 μm.

Scratching of the coating surface with the diamond indenter resulted in cohesive fracture of the coating at a load of 93.4 N and adhesive fracture at a load of 185.3 N. The adhesive fracture has the mechanism of plastic pushing off and impression of the coating material into the aluminium substrate. No brittle fracture was observed.

The coating had low porosity (< 1 %) and high adhesion and cohesion strength. It can be used to protect aluminium structures from corrosion and wear.

REFERENCES

[1] V.V. Sadkov, I.I. MirkinTekhnologiyaLyogkikhSplavov, 2006, No4, P. 168-174.
[2] S. Karimova, Nauka I Zhyzn,No6, 2007.

[3] A.A. Iljin, S.V. Babin,TekhnologiyaLyogkikhSplavov, 2006, No1, P. 202-207.
[4] J. Kawakita, S. Kuroda, T. Fukushima, H. Katanoda, K. Matsuo, J. Kitakyushu,Surf. Coat. Tech.,2006, Vol. 201, No (3–4), P. 1250-1255.
[5] K. H. Kim, M. Watanabe, K. Mitsuishi, J. Kawakita. ITSC 2008.
[6] R.E. Blose, ITES, 2005.
[7] A. Rezaeian, R. Chromik, S. Yue, E. Irissou and J.-G. Legoux, ITSC, 2008.
[8] Fr.-W. Bach, D. Hannover, K. Möhwald and D. Kolar, D. Witten, ITSC, 2005.
[9] Yu.N Tyurin, O.V. Kolisnichenko, I.M. Duda, UprochnyayushchieTekhnologii I Pokrytiya,2009, No5, P. 27-33.
[10] C.J. Li, A. Ohmori, Y. Harada,Therm. Spr. Tech., 1996,Vol. 5, No1, P. 69-73.
[11] E.A. Levashov, D.V. Shtansky,UspekhiKhimii, 2007,Vol. 76, No5, P. 501-509.
[12] H.E. Hintermann, Fresenius J Anal. Chem. B., 1993, Vol. 346, P. 45-52.
[13] Q.R. Hou, J. Appl. Phys, 1999, Vol. A 68, P. 343–347.
[14] X.Q. Ma, D.W.Gandy,ITSC, 2008.
[15] J. Karch, Birringer, H. Gleiter, Nature**,** 1987, Vol. 330**,** P. 556 – 558.